JOURNAL OF FOREST SCIENCE, *58*, 2011 (6): 287–297

The use of hyperspectral remote sensing for mapping the age composition of forest stands

O. Skoupý[1], L. Zejdová[1], J. Hanuš[2]

[1]*Department of Geoinformation Technologies, Faculty of Forestry and Wood Technology, Mendel University in Brno, Brno, Czech Republic*

[2]*Global Change Research Centre AS CR, Brno, Czech Republic*

ABSTRACT: The paper deals with the issue of mapping the age composition of stand groups using hyperspectral imagery acquired by the AISA Eagle VNIR sensor in the Bílý Kříž locality in the Moravian-Silesian Beskids Mts. An object-oriented approach was employed through segmentation and subsequent classification by means of Nearest Neighbour (NN) algorithm in the environment of eCognition Developer 8 and artificial neural network (ANN) classification provided by ENVI 4.7 software. Because of the dominant occurrence of Norway spruce (*Picea abies* [L.] Karst.) monocultures in the studied locality the work focuses primarily on the distinguishability of two selected age classes of Norway spruce (10–20 years and 70–80 years). It studies possibilities of a more detailed age estimation of stand groups aged from 10 to 80 years based on the classification into the boundary classes, which shows similarity to dithering based on random algorithm. Comparison with the outline map of the Forest Management Plan shows a correlation (r^2 = 0.83) between the spectral characteristics of Norway spruce stands and their age composition.

Keywords: age classification; forestry; hyperspectral; object oriented; segmentation; spruce

At present remote sensing of the Earth is one of the most rapidly developing methods dealing with the mapping of the Earth's surface. Its advantage consists in the rapid acquisition and subsequent processing of data, which facilitates a nearly instant creation of up-to-date maps of extensive areas. With advance of time and with the progressing specialization of use, remote sensing of the Earth and aerial photogrammetry proceed towards increased resolution – both spatial and spectral (Elachi, van Zyl 2006). Thus, another technical branch of remote sensing has been emerging in the last three decennia, which is referred to as aerial and satellite spectrometry (Goetz 2009). It is coming to existence was motivated by the presumption of an improved identification of particular spectral attributes of individual materials through the more detailed sensing and mapping of the spectral reflectance curve (Wulder et al. 2003). This expectation was supported by results of geological applications mapping the mineral composition (Van Der Meer, 1994) and in the case of forestry by the ascertainment of the specific spectral features of canopy chemistry (Zagolski et al. 1996; Martin, Aber 1997).

At present, the centre of research into the employment of imaging spectrometry focused on forestry consists in ecological applications (Rautiainen et al. 2010). The research relies primarily on the physical approach and on quantitative analyses (Malenovský et al. 2009; Lukeš et al. 2010), which make it possible to explore the condition of studied stands through the contents of substances on the basis of radiative transfer models. Regard-

Supported by the Internal Grant Agency Project IGA LDF, Project No. 18/2010 "Use of hyperspectral imagery for forestry mapping", and by the Ministry of Education, Youth and Sports of the Czech Republic, Project No. MSM 6215648902 "Forest and Wood – Support to a functionally integrated forest management".

ing the exigency of the quantitative approach, the practical broader applicability of hyperspectral aerial images is currently confined rather to qualitative analyses, namely to the classification of the species composition of forest stands based on the empirical approach, particularly through comparing signatures of individual pixels of the image with libraries proposed by Clark (2003). With respect to the problematic calibration of data and absence of distinct spectral attributes of individual woody plants, the most reliable source of libraries for the application of this procedure in forestry can be seen in training sets obtained from the *in situ* measurements.

This paper will focus on the practical applicability of imaging spectrometry for quantitative analyses and will suggest an effective and easy-to-replicate methodology, which makes use of tools commonly available in the field of aerial imagery processing. In particular, it will deal with the classification of the species and age composition of forest stands, and in the case of Norway spruce also with the quantification of age value based on the mutual proportion of classified objects occurring in the studied territory with considering the classification as random dithering. Thus acquired data may be in principle subsequently applied a reverse procedure (Discepoli, Gerace 2004) and more detailed age values can be retroactively interpolated. On the grounds of empirical approach, the work aims to demonstrate dependence between the species and age compositions of stands and their spectral characteristics.

Hyperspectral remote sensing and the species and age classification of forest stands

The first attempt at an identification of tree species based on leaf contents of nitrogen and lignin was that by Wessman et al. (1988). A more recent practical application of the hyperspectral approach, in this case for mapping the species composition of coniferous tree species, was by Gong et al. (1997). Pu (2009) studied the mapping of forest stands species composition also for the broadleaved tree species. In his works, the author makes use namely of linear discriminant analysis (LDA) and neural network analysis (NNA) in which he achieves the accuracy of classification above 80%. Distinguishability of tree species even within the same genus was demonstrated van Aardt and Wynne (2007), who discerned individual *Pinus* species with a relatively high reliability.

The increasing resolution of hyperspectral data in the last decade has led to efforts for the implementation of an object-oriented approach and mapping at the level of crowns. In their work concerning the classification of rainforest species composition with using 30 spectral bands and the object-oriented approach, Clark et al. (2005) reached the total accuracy of 86%. The classification of objects representing the crowns of individual trees must be preceded by image masking and segmentation. Among researchers dealing with the issue are e.g. Brandtberg and Walter (1998), Culvenor (2002) or Bunting and Lucas (2006).

Buddenbaum et al. (2005) studied the age composition classification of coniferous stands in the western part of Germany for which they used a combination of spectral and textural characteristics. Applying hyperspectral data only, they achieved the 66% accuracy of classification using Spectral angle mapper (SAM) and Maximum likelihood (MLE) classifiers.

The question of quantifying the stand age value is disputable especially with regard to the fact that the most of the vegetation cover spectral response is provided by foliage, which is logically younger than the age of individual trees. Their age is difficult to ascertain even by non-invasive ground methods (Franklin 2001). The direct correlation between the stand age and the spectral response established by remote sensing approximates the classical "nonsense" correlation (De Wulf et al. 1990). Cohen et al. (1995) found out a dissimilar spectral response of broad age classes, which however resulted rather from different structure that showed in different illumination, absorption and shadows corresponding to different size and density of trees (Gemmell 1995). In very young and homogeneous stands, we can find a strong dependence between age and reflectance scanned by Landscat TM (Fiorella, Ripple 1993). Considering a higher spatial and spectral resolution of data in this work, which makes it possible to eliminate to a certain extent most of the above-mentioned factors by means of masking and object-oriented approach, we get closer to answering the question whether it is possible to determine the age of stands on the basis of the reflectance of individual tree crowns, in this case the age of spruce stands covered by the available imagery. One way or another, it is necessary to bear in mind that the non-invasive direct measurement of the age value is impossible; what we can measure are manifestations that are its consequence (Cohen et al. 1995) and may be unique for each locality like for example the history of stress.

MATERIAL AND METHODS

The basic material used was an archive aerial hyperspectral image acquired in 2006 in the Bílý Kříž locality in the Moravian-Silesian Beskids. Data covering an area of ca 2 km^2 were taken by the AISA Eagle sensor at a resolution of 0.4 m on 14 September 2006 – altogether 65 bands within a spectral range of ca 400–1,000 nm. Geometric and atmospheric corrections of the images have been performed by experts from the Institute of System Biology and Ecology ASCR.

The locality lies within approx. coordinates 18°54'E, 49°50'N at an altitude of 750–950 m a.s.l. The mean annual air temperature is 5.5°C and the mean annual precipitation amount ranges from 1,000 to 1,400 mm. Snow cover persists at the highest elevations for 160 days in the year.

The area is characterized by pure stands of Norway spruce (*Picea abies* [L.] Karst.) with admixed broadleaves; most often represented is European beech (*Fagus sylvatica*), less abundant is goat willow (*Salix caprea*), silver birch (*Betula pendula*) and individually occurring is also the silver fir (*Abies alba*) (Urban et al. 2007).

Ground measurements by the GPS apparatus consisting of the instrument Model Trimble GeoExplorer Geo XT with the Trimble Tornado antenna were made in the locality on 22 September 2010. The ground campaign served to collect data by means of points and polygons for the determination of training sets. The collection of data covered continuous even-aged Norway spruce stands and solitary broadleaves. The time lag between the acquisition of hyperspectral image and the ground measurement has been taken into consideration when estimating stand ages during the field measurement, where four years were automatically subtracted from estimated ages.

Groundwork for the evaluation of age class classification accuracy was chosen to be an outline map of the Forest Management Plan (FMP) 2008 available on the WMS server operated by the Forest Management Institute (ÚHÚL Brandýs nad Labem). Vectorization of lines was followed by the creation of a polygonal map featuring the layout of stand groups in the studied locality with the values of their age classes.

Software used includes namely the ENVI 4.7 programme for masking and classification by means of artificial neural networks, eCognition Developer 8 for segmentation and classification by means of Nearest Neighbour algorithm and ArcGis 10 for the preparation of the FMP outline map, necessary modifications of layers and visualization.

Masking of non-vegetation pixels

Based on the high resolution of the obtained images, we proceeded to the object-oriented approach and to the supervised classification. The first step in data processing was a reduction of the number of bands and masking out of noise pixels. Regarding the low image signal/noise ratio, six bands in the shortest wavelengths (392–435 nm) where the spectral response of the vegetation was weakest had to be eliminated from the classification and the selection for the classification included only the pixels whose reflectance curve was not distorted by noise. These were chiefly the pixels that were automatically assigned pre-adjusted values in the visible range of electromagnetic spectrum (0.25% reflectance in the area of blue and red bands, 0.50% reflectance in the area of green bands).

The subsequent image segmentation into the crown level of individual trees refrains from the traditional procedure (Brandtberg 1998) using the image smoothing in the first step. Instead of the elimination of noise pixels and reduction of data volume the procedure used was based on the following hypothesis:

Considering the character of vegetation cover insolation, the purest signal with the highest reflectance values can be expected on the tops of tree crowns. Thus, each individual represents a local maximum, which is surrounded by pixels of lower reflectance (non-insolated and shaded parts of crowns) and often also by a mixed signal (canopy gaps where the foliage of two or more individuals reaches into one pixel). If an adequate threshold value of minimum reflectance is established and all pixels not reaching the value in selected bands are masked out, it is possible to create an image that will contain only clusters of pixels representing crown tops of individual trees.

Supposed benefits of this approach are as follows: material reduction in the volume of processed data and masking out most of mixed pixels. Classification is made only on pixels with the strongest and cleanest signal. Another benefit is markedly simplified and advanced segmentation.

Because only the pixels on insolated crown parts directly enter the classification, the problem of different results on insolated and non-insolated slopes is largely resolved in spite of the fact that the crowns of trees on the reverse slopes will be rep-

resented by smaller clusters in the image than the crowns of similarly grown-up trees on the forward slopes. The threshold value should therefore be chosen also in dependence on the elevation angle of the sun at the time of sensing and on the maximum gradient of slopes with the opposite exposure.

Based on the assessment of multiple results, the threshold value for masking was selected to be 1% over bands from 444 nm to 498 nm. Each pixel that did not reach the value in any of the bands was masked out.

The following step was the application of another mask to reduce the volume of processed data. This time, it was on the basis of a vegetation index in order to eliminate all non-vegetation pixels that would not be used in the classification focused on the species and age composition of stands. The Normalized Difference Vegetation Index (NDVI) was selected. The threshold value was chosen to be 0.8, at which a maximum of pixels not belonging to forest areas (except for grass stands and shrubs) was eliminated with no simultaneous essential loss of data in the stands. The resulting raster delimited the individual crowns satisfactorily (the ideal state of isolated pixel clusters was achieved especially in Norway spruce stands over 70 years – see Fig. 1) without the tree tops on the reverse slopes having been masked out. More continuous clusters of pixels representing multiple crowns were formed chiefly on insolated slopes, in younger stands, in groups of individual broadleaves with a continuous canopy and particularly in marginal individuals.

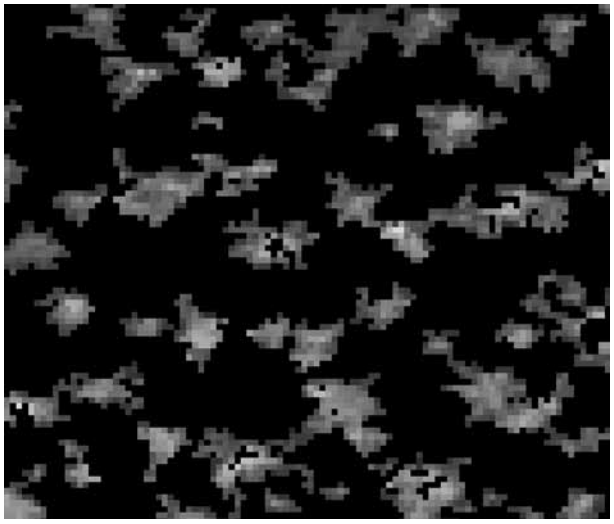

Fig. 1. Results of masking out unused pixels on the basis of reflectance and NDVI in a Norway spruce stand aged 70 to 80 years

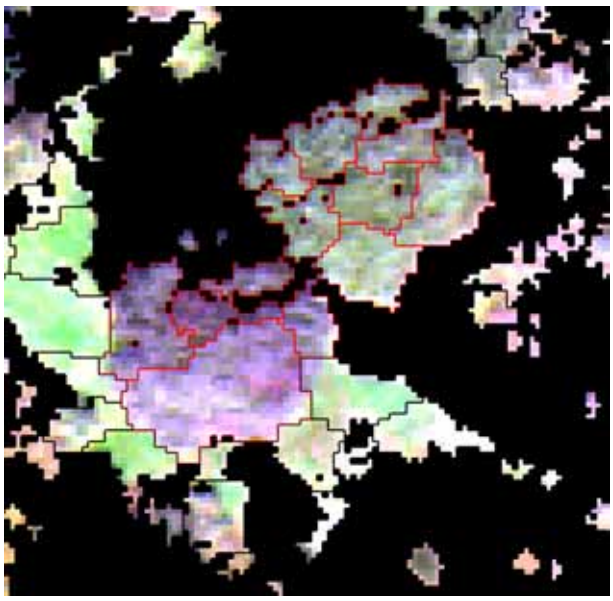

Fig. 2. Example of the segmentation result on two broadleaved trees that have also been selected as control sets for Class BS

Image segmentation into the level of individual crowns

After masking out pixels non-utilizable for the classification, we proceeded to the image segmentation. We selected multilevel (multiresolution) segmentation on the basis of one layer (444 nm) that showed the best prerequisites for successful segmentation even in the case of linked clusters representing individual tree tops (most contrasted transitions) between individual crowns. The scale parameter (Baatz et al. 2004) was adjusted at 20. Parameters for shape and compactness were adjusted on the basis of a presumption that within a great amount of weakly associated pixel clusters representing the individual tree crowns, the crowns themselves will be plotted exactly as the largest possible compact pixel clusters in the image with minimum regard of spectral characteristics. This is why the compactness parameter ensuring the roundness of resulting shapes was assigned the maximal value possible (1.0) and the shape parameter which determines how much the shape characteristics will be favoured over spectral properties was set up at 0.8. The resulting objects meet the required results to a maximum possible extent. As to bulky crowns, namely in broadleaved trees (classified as BS), one crown is often covered by several objects (see Fig. 2). Nevertheless, a general rule applies that the accuracy of segmentation increases with the increasing age of the stands, i.e. with more open canopy and lower interconnection of individ-

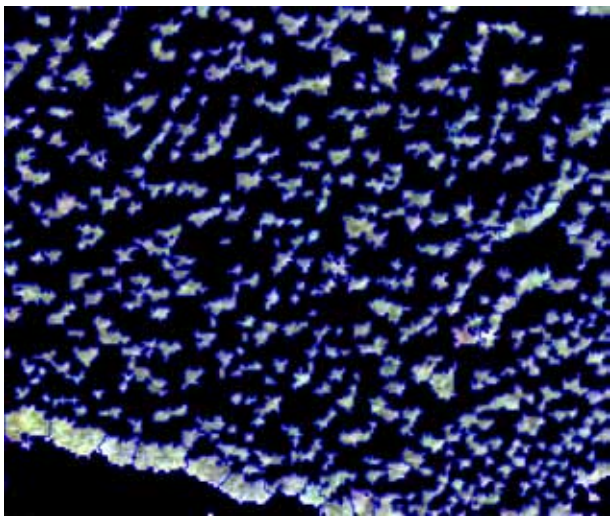

Fig. 3. Example of the segmentation result in a Norway spruce stand aged 20–30 years

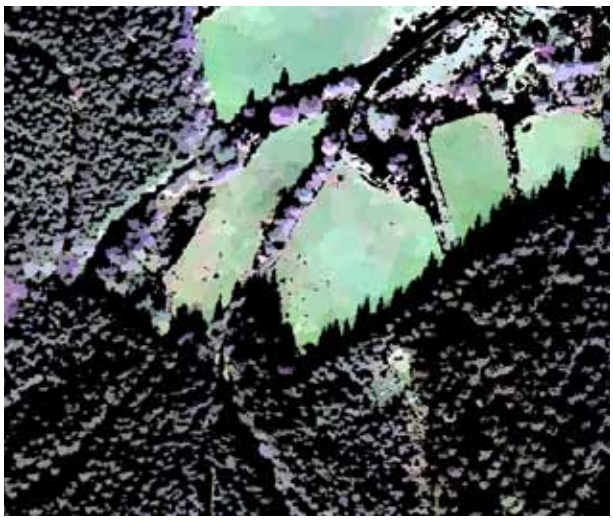

Fig. 4. Segmented image, individual pixels are assigned the average reflectance values of the respective objects

ual clusters, and the result approximates an ideal condition when the number of clusters roughly corresponds to the number of individuals. An example of the segmentation result in a stand aged 20–30 years is presented in Fig. 3.

The following step was the elimination of inadequately small-sized objects in which mean reflectance values for individual bands were calculated from a low amount of pixels, and which could therefore be loaded with error that had a potential to negatively affect the resulting classification especially in cases when such objects were parts of training sets. For these reasons, all objects represented by less than 5 pixels (0.8 m^2) were excluded from further processing. The segmented image was exported in the raster format and the table of attributes for each object contained the mean values of objects in individual bands. This vector set was used to create 59 raster layers, which were sequenced to give a new hyperspectral image. An advantage of the new image is that it represents a combination of the object-oriented and per-pixel approach to classification when all pixels belonging to one object are always going to be allocated to the same class. Part of the segmented image where each pixel of an object is assigned its respective mean value can be seen in Fig. 4.

Segmented image classification using the NN algorithm

The test classification whose basic parameters (training and testing sets) were subsequently used also in the classification by means of neural networks in the ENVI 4.7 environment was conducted in the environment of eCognition Developer 8 software. Regarding the low representation of broadleaved species in the stands and their diversity, it was impossible to obtain a sufficient amount of training and control sets for individual species so that the result would be statistically significant. This is why all broadleaved trees were classified into one class BS (broadleaved species). Other two classes include Norway spruce stands of two age classes (in our case, age classes denote decennial intervals of stand age): second age class (10 to

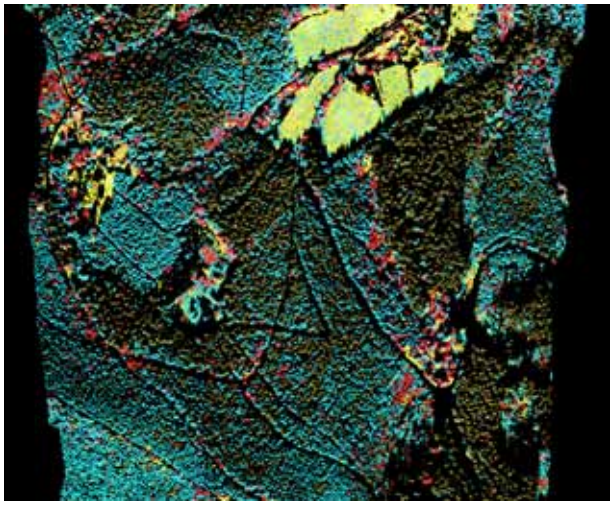

Fig. 5. Results of the NN classification in the programme eCognition Developer 8 on a part of the studied area. Cyan and brown are objects classified in SSY and SSO classes. See the gradual change in the proportion of SSY and SSO objects occurring in the locality in dependence on the age of spruce stands. Red and yellow are objects in classes BS and OS, respectively

20 years) and eighth age class (70–80 years). For these two classes we chose working names SSY (young spruce stand) and SSO (old spruce stand). Other conifers in the locality were neglected due to their very scarce occurrence. All other surfaces not belonging to forest stands (namely permanent grass stands) were classified in the last class OS (other surfaces). The reason for specifying two classes of spruce stands was our effort to find out whether the age class of the given group of stands can be estimated on the basis of the mutual ratio of SSY and SSO objects occurring on individual plots. With respect to the similarity of spectral reflectance curves in the spruce stands of different age classes, we expected that with the increasing age, the proportion between the number of objects classified in SSY and SSO classes would be gradually changing from young stands with the dominant SSY class to old stands with the dominant SSO class.

Training sets for the SSY and SSO classes were determined on the basis of *in situ* surveyed polygons delimitating continuous even-aged spruce stands without admixed broadleaves. Within a surveyed polygon, all objects were selected that were included in the training set of a particular class. Training sets of Class BS consist of individual broadleaved trees surveyed by the GPS point measurement. Using these coordinates, single objects representing the respective crowns were collected in the image and were subsequently denoted as training sets. With respect to their distinguishability by eye, training sets of Class OS were determined only by comparison with the orthophotomap. A similar method was used to select the objects of the control sets. When the training sets had been determined, it was possible to proceed to the proper classification based on the nearest neighbour algorithm. The classification was calculated from mean reflectance values of individual objects in all 59 bands in the range from 444 to 982 nm. Classification accuracy was evaluated through the calculation of error matrix based on the agreement of the object classification with the control sets. An example of the classification results can be seen in Fig. 5.

Image classification using the artificial neural networks (ANN)

As an alternative comparison method of classification we chose the application of an artificial neural network (ANN) in the ENVI 4.7 programme. The reason for its implementation was expected greater flexibility than in other offered classifiers considering the fact that the classification was not targeted at the recognition of particular spectral attributes. Training and control sets used in this method were identical to those in the classification using the NN algorithm.

The classification was carried out by applying a layered feed-forward perceptron artificial neural network. Several network trainings were performed in search of optimal parameters. The best results were reached when the sigmoidal (logistic) activation function of neurons with the threshold value (Training Threshold Contribution) was selected to be 0.9, the training momentum was adjusted at 0.9, the training rate was set up as 0.05 and the total number of iterations was adjusted at 500 (RSI 2004). With these values, the network error (RMS error) gradually converged to 0.13.

Quantification of age values

The tool selected for the evaluation of achieved accuracy in the classification of the age classes of spruce stands was a comparison with data in the FMP 2008 outline map from which a map of age classes for individual groups of stands was created.

The accuracy of determination of the age composition of spruce stands was checked on the basis of a normalized index. A prerequisite for the establishment of the index is an attempt at the additional quantification of the variable of age based on a qualitative analysis. The result of classification shows characteristics similar to dithering based on the random algorithm as described in Velho et al. (2009), which is in this case seeded largely by noise in the image data and by the error of the classification itself. Thus, in the case of assumed unambiguous distinguishability of young and old spruce stands, the classification into the two classes would lose the characteristic of thresholding and the original values above which the classification into the limit classes was made can be retroactively estimated based on the law of large numbers. The prerequisite is however a sufficient number of objects on the surveyed surface, in our case extensive groups of stands.

In order to compare the age index with actual values, a vector map was created of age classes acquired from the FMP outline map. It was subsequently converted into the raster format (at a resolution of 0.4 m, corresponding to the resolution of the classified data) and a table was generated using the Combine tool, which recorded the number of pixels allocated to the respective classes occurring

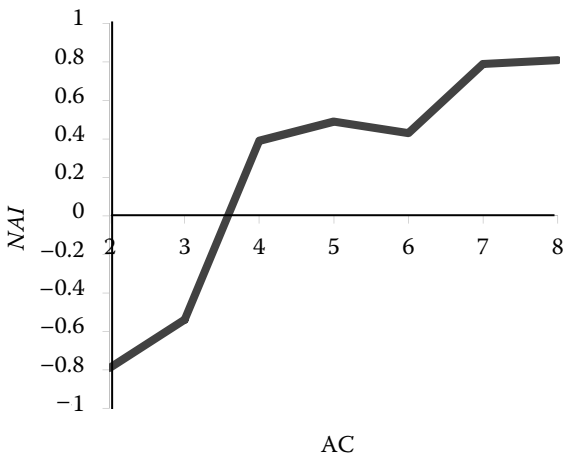

Fig. 6. Relation between the value of Normalized Age Index (*NAI*) obtained from the classification and the age class designation (AC) obtained from the FMP outline map

on all plots falling in a certain age class (according to the FMP outline map).

Subsequently, a calculation was made of normalized indices for age classes (AC) 2–8 from the following equation:

$$NAI_n = \frac{A_n - B_n}{A_n + B_n}$$

where:

NAI_n – the index calculated for groups of stands classified in the nth age class,

A_n – the total number of pixels classified as SSO on all plots mensurated as class *n*,

B_n – the analogical value for all pixels classified as SSY.

The obtained indices were edited in tabular form and converted into graphs. Based on the table, a correlation coefficient was calculated between the mensurated age of the groups of stands obtained from the FMP map and the value gained from the *NAI* index calculation. The final step to visualize the estimated age of the individual groups of stands consisted in the creation of a map where *NAI* was calculated for each group of stands based on the proportion of areas classified in SSY and SSO classes. Age class (AC) values of individual groups of stands were estimated from the obtained *NAI* on the basis of linear regression.

RESULTS

Based on the comparison of classification results with the control sets, aggregate classification accuracies were established for the NN (0.88) and ANN (0.92) classifiers – see Tables 1 and 2. It was shown that as compared with the control sets and after the error matrix calculation, the method of classification provided more accurate results using ANN in the ENVI 4.7 software compared to the NN classification in the eCognition Developer 8 environment. However, both methods of classification introduced a relatively high omission error of BS class. At the same time it was demonstrated that older Norway spruce individuals were classified in the SSY class more frequently than younger individuals in the SSO class. The correlation coefficient between the area-weighted average of normalized

Table 1. Error matrix of classification by the NN method (units are objects)

User class\Sample	BS	SSY	SSO	OS	Sum
BS	60	28	7	8	103
SSY	4	767	70	6	847
SSO	1	119	711	0	831
OS	2	7	1	351	361
Unclassified	0	0	0	4	4
Sum	67	921	789	369	2,146
Producer	0.90	0.83	0.90	0.95	
User	0.58	0.91	0.86	0.97	
Overall Accuracy	0.88				
KIA	0.82				

BS – broadleaved species, SSY – young spruce stand, SSO – old spruce stand, OS – other surfaces, KIA – Kappa index of agreement

Table 2. Error matrix of classification by the ANN method (units are pixels)

User class\Sample	BS	SSY	SSO	OS	Sum
BS	9,295	2,093	342	1,587	13,317
SSY	448	52,792	1,819	318	55,377
SSO	60	2,103	31,888	0	34,051
OS	0	504	0	66,712	67,216
Unclassified	0	0	0	197	197
Sum	9,803	57,492	34,049	68,814	170,158
Producer	94.82	91.82	93.65	96.95	
User	69.80	95.33	93.65	99.25	
Overall Accuracy	0.92				
KIA	0.94				

BS – broadleaved species, SSY – young spruce stand, SSO – old spruce stand, OS – other surfaces, KIA – Kappa index of agreement

Table 3. Area-weighted average and dispersion of calculated *NAI* values for stands of the same age class (AC) according to the FMP outline map

AC	*NAI*	Dispersion
2	–0.79	0.06
3	–0.54	0.29
4	0.39	0.03
5	0.49	0.04
6	0.43	0.07
7	0.79	0.02
8	0.81	0.01

age index values calculated for all plots of the given age class (AC) and the values from the FMP outline map is 0.91 (r^2 = 0.83). The highest variance in calculated *NAI* occurs at the 3rd age class (20–30 years) and equals 0.29. The relation between *NAI* values calculated from the classification results by ANN and age classes obtained from the FMP outline map is illustrated in Fig 6, numerical values along with dispersion in *NAI* calculation for the respective age classes can be found in Table 3. If a simple linear dependence between age and spectral response is presumed, the area-weighted average of deviations between the stand age class value and the stand age class estimated from *NAI* equals 0.98. The highest deviations occur at intermediate age classes, where the age value is systematically underestimated (the maximal weighted average of deviations occurs in the 4th age class and equals 2.18, i.e. 21.8 years). The AC values estimated from the calculated *NAI* and AC values harvested from the FMP outline map can be compared in Fig. 7.

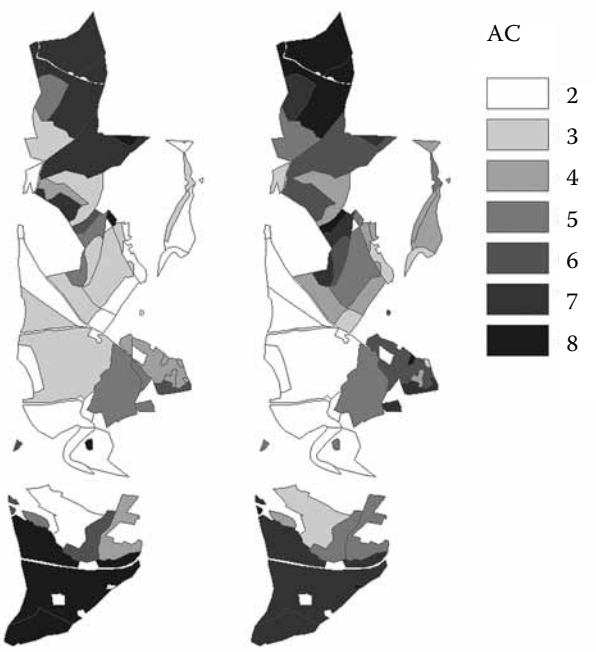

Fig. 7. Comparison of AC values obtained from the FMP outline map (left) with AC values estimated using *NAI* (right)

DISCUSSION

The two employed methods of classification demonstrated that the age of spruce stands can be distinguished on the basis of spectral characteristics. The result may be partly due to different spectral characteristics of crowns and partly due to some other factors such as the decreasing visibility of unshaded undergrowth with the increasing age (Franklin 2001). The comparison of results suggests that ANN can be recommended as a more suitable classifier than NN even though the data conversion is laborious because the compatibility

between the employed types of software is low. This can possibly be avoided for example by the use of the ENVI Feature Extraction Module instead of the eCognition. Acquiring and testing the module for the segmentation purposes may be suggested as a subject for future work. The relatively large omission error in the case of BS class in both classifications was likely to have resulted from the uneven interspersion of broadleaved species particularly into the young spruce stands and their inclusion in training and control sets. Taking into account the distribution of SSY and SSO objects on the plots of intermediate age classes, ANN approximates thresholding more than NN, which corresponds to its higher accuracy provided that the age of stands, i.e. concomitant phenomena accompanying the ageing of stands, can be discerned (Franklin 2001).

The result of the classification by means of artificial neural networks suggests that the gradient of the change in stand spectral characteristics decreases with the increasing age of the stands with the greatest changes being observed to occur ca between the 3rd and 4th age class. Looking at Fig. 1 we can see that in plots mensurated in the sixth age class, this trend is disturbed, most probably due to the low amount of data and because of non-homogeneous species and age composition of stands on the concerned plots. Individual groups of stands of the third age class exhibit the greatest dispersion of the calculated *NAI*, which corresponds to the assumed nonlinear dependence between the age and spectral reflectance with the most significant changes occurring between 30 to 40 years of age. Therefore, in the case of 3rd age class groups of stands the highest deviations occur between the assumed AC estimated from *NAI* based on the simple linear regression and AC obtained from the FMP outline map. The errors relate mainly to one particular locality in which a possible FMP data error or a gross mistake of the enumeration officer can be considered with respect to stand characteristics that rather correspond to older age classes. The information in the FMP outline map itself may not correspond to actual age; the groups of stands may be reclassified into other AC according to their actual condition. At the same time, it is necessary to take into account that one age class represents a relatively wide interval of 10 years and the difference in ages as well as in the spectral response of individuals classified in the same class may thus be considerably higher than the difference in ages of individuals classified in neighbouring AC. Another factor that could be a source of errors is the two years gap between the FMP mapping and image acquisition, namely the stress history. However, due to a relatively small testing area and no extreme weather events occurring at the site during the relatively short period, this factor was not considered significant.

The assumption of linear dependence when estimating the age values of individual stands is not of course ideal and imposes a significant error on the estimation of results. If there is any systematic dependence between stand age and its spectral response, it should be possible to determine a function for the more accurate estimation of stand ages. However, this cannot be done for this single case on the basis of one hyperspectral image. Finding any universally applicable function would be a result of numerous applications of this methodology in various conditions. Of course, there is always a possibility to estimate the function for each particular case if the ground measurement defines training sets for each age class, but this would lead to increasing demands on the methodology thus compromising its effectiveness.

In spite of relatively optimistic results, namely when considering the dispersion in calculated *NAI*, the applicability of the methodology needs to be verified on another set of data from a different locality. Based on those data, a map will be created of the age of groups of stands that will be subsequently compared with the corresponding stand map. A successful creation of the map of age classes of the groups of stands calls for the development of a reverse tool such as image segmentation at a smaller scale where potential groups of stands can be delimited by detected breaklines and then assigned the age values calculated from the *NAI*. The applicability of this method increases with the increasing amount of distinct, mainly straight lines in the landscape matrix. Another employable tool is a convolution filter for the calculation of *NAI*, through which the age value is estimated for individual pixels of the resulting map separately. This method could be used in the case of stands with smoother transitions between larger groups of stands.

It should be noted that with respect to the low spectral diversity of neighbouring age classes, the proposed methodology cannot be used to determine the age of particular individuals. It can be employed for mapping the age composition of stands consisting of even-aged groups of stands or for estimating the average age of uneven-aged stands.

CONCLUSION

Our research implementing the object-oriented approach and site-specific supervised classification

demonstrated a high rate of correlation between the spectral characteristics of stand reflectance and stand age class in the Norway spruce groups of stands aged 10–80 years. Accuracies achieved by the Nearest Neighbour algorithm and by the use of the artificial neural networks in classifying individual Norway spruce specimens into two classes representing Age Class 2 and Age Class 8 were 86% and 96%, respectively. With the inclusion of the two remaining classes (broadleaved species and other surfaces), the classification accuracy was 88% (NN) and 92% (ANN).

The proposed methodology of object-oriented approach can be applied in the analysis of the species and age composition of forest stands under condition of the increasing availability of high-quality hyperspectral imagery of submeter resolution. Also the wider applicability of the methodology should be tested in other than pure Norway spruce stands, especially when considering the difficulties with segmentation of broadleaf stands. Even when considering just Norway spruce stands, the methodology still calls for further testing in different conditions where its validity could be confirmed. In such a case, the presumed generally applicable function of dependence of the spectral response on stand age could be then approximated to provide more accurate results.

Regarding the problematic data pre-processing and calibration, the supervised classification continues to be a method yielding the most reliable results in using imaging spectrometry for forest applications, which usually compensate for the necessity of optimizing the methodology for particular cases and ground measurement of the training sets.

References

Baatz M., Benz U., Dehghani S., Heynen M., Höltje A. (2004): eCognition Elements 4.0 User Guide. München, Definiens Imaging: 71.

Brandtberg T., Walter F. (1998): Automated delineation of individual tree crowns in high spatial resolution aerial images by multiple-scale analysis. Machine Vision and Applications, ***11***: 64–73.

Buddenbaum H., Schlerf M., Hill J. (2005): Classification of coniferous tree species and age classes using hyperspectral data and geostatistical methods. International Journal of Remote Sensing, ***26***: 5453–5465.

Bunting P., Lucas R. (2006): The delineation of tree crowns in Australian mixed species forests using hyperspectral Compact Airborne Spectrographic Imager (CASI) data. Remote Sensing of Environment, ***101***: 230–248.

Clark R.N., Swayze G.A., Livo K.E., Kokaly R.F., Sutley S.J., Dalton J.B., McDougal R.R., Gent C.A. (2003): Imaging spectroscopy: Earth and planetary remote sensing with the USGS Tetracorder and expert systems. Journal of Geophysical Research, ***108***: 1–44.

Clark M.L., Roberts D.A., Clark D.B. (2005): Hyperspectral discrimination of tropical rain forest tree species at leaf to crown scales. Remote sensing of environment, ***96***: 378–398.

Cohen, W.B., Spies T.A., Fiorella M. (1995): Estimating the age and structure of forests in a multiownership landscape of western Oregon, USA. International Journal of Remote Sensing, ***16***: 721–746.

Culvenor D.S. (2002): TIDA An algorithm for the delineation of tree crowns in high spatial resolution remotely sensed imagery. Computers & Geosciences, ***28***: 33–44.

Discepoli M., Gerace I. (2004): Inverse dithering through IMAP estimation. In: Lagana A., Gavrilova M.L., Kumar V., Mun Y., Tan J.K, Gervasi O. (eds): Proceedings, part IV of the Computational Science and Its Applications – ICCSA 2004. Assisi, 14.–17. May 2004. London, Springer: 379–388.

De Wulf R.R., Gossens R.E., De Roover B.P., Borry F.C. (1991): Extraction of forest stand parameters from panchromatic and multispectral SPOT-1 data. International Journal of Remote Sensing, ***11***: 1571–1588.

Elachi C., van Zyl J. (2006): Introduction to the Physics and Techniques of Remote Sensing. 2nd Ed. Hoboken, Wiley-Interscience: 552.

Fiorella M., Ripple W. J. (1993): Determining the successional stage of temperate coniferous forest with landsat satellite data. Photogrammetric Engineering & Remote Sensing, ***59***: 239–246.

Franklin S.E. (2001): Remote Sensing for Sustainable Forest Management. Boca Raton, Lewis: 407.

Gemmell F.M. (1995): Effects of forest cover, terrain and scale on timber volume estimation with thematic mapper data in a rocky mountain site. Remote Sensing of Environment, ***51***: 291–305.

Goetz A.F.H. (2009): Three decades of hyperspectral remote sensing of the Earth: A personal view. Remote Sensing of Environment, ***113***(Supplement 1): 5–16.

Gong P., Pu R., Yu B. (1997): Conifer species recognition: An exploratory analysis of in situ hyperspectral data. Remote Sensing of Environment, ***62***: 189–200.

Lukeš P., Malenovský Z., Kaplan V., Hanuš J., Homolová L. (2010): Estimation of Norway spruce leaf chlorophyll content from CHRIS/PROBA satellite image data. In: Lacoste-Francis H. (ed.): Proceedings of the Hyperspectral workshop 2010. Frascati, 17.–19. March 2010. Noordwijk, ESA ESRIN: 1–4.

Malenovský Z., Lukeš P., Kaplan V., Hanuš J., Homolová L. (2009): Multi-scale aproaches retrieving norway spruce leaf chlorophyll content from high spatial resolution air-/space borne spectral image data. In: Pro-

ceedings of the Workshop on the Retrieval of Geophysical Variables Using High Spatial Resolution Optical Imagery. Noordwijk, 14.–15. October 2009. Noordwijk, ESA/ESTEC: rozsah stran.

Martin M., Aber J. (1997): High spectral resolution remote sensing of forest canopy lignin, nitrogen, and ecosystem processes. Ecological Applications, *7*: 431–443.

Pu R. (2009): Broadleaf species recognition with in situ hyperspectral data. International Journal of Remote Sensing, ***30***: 2759–2779.

Rautiainen M., Heiskanen J., Eklundh L., Mottus M., Lukeš P., Stenberg P. (2010): Ecological applications of physically based remote sensing methods. Scandinavian Journal of Forest Research. ***25***: 325–339.

RSI (2004): ENVI User's Guide, ENVI 4.1 September 2004 Edition. Boulder, Research Systems, Inc.: 1150

Urban O., Janouš D., Acosta M., Czerný R., Marková I., Navrátil M., Pavelka M., Pokorný R., Šprtová M., Zhang R., Špunda V., Grace J., Marek M.V. (2007): Ecophysiological controls over the net ecosystem exchange of mountain spruce stand. Comparison of the response in direct vs. diffuse solar radiation. Global Change Biology ***13***: 157–168.

Aardt J.A.N. Van, Wynne R.H. (2007): Examining pine spectral separability using hyperspectral data from an airborne sensor: An extension of field-based results. International Journal of Remote Sensing, ***28***: 431–436.

Meer F. Van der (1994): Extraction of mineral absorption features from high-spectral resolution data using non-parametric geostatistical techniques. International Journal of Remote Sensing, ***15***: 2193–2214.

Velho L., Frery A.C., Gomes J. (2009): Image Processing for Computer Graphics and Vision. 2nd Ed. London, Springer-Verlag: 462.

Wessman C.A., Aber J.D., Petersen D.L., Melillo J.M. (1988): Remote-sensing of canopy chemistry and nitrogen cycling in temperate forest ecosystems. Nature, ***335***: 154–156.

Wulder M.A., Franklin S.E. (2003): Remote Sensing of Forest Environments: Concepts and Case Studies. Boston, Kluwer Academic Publishers: 519.

Zagolski F.P., Pinel V., Romier J., Alcayde D., Fontanari J., Gastellu-Etchegorry J. P., Giordano G., Marty G., Mougin E., Joffre R. (1996): Forest canopy chemistry with high spectral resolution remote sensing. International Journal of Remote Sensing, ***17***: 1107–1128.

Received for publication November 2, 2011
Accepted after corrections April 23, 2012

Corresponding author:
Ing. Ondřej Skoupý, Mendel University in Brno, Faculty of Forestry and Wood Technology, Department of Geoinformation Technologies, Zemědělská 3, 613 00 Brno, Czech Republic
e-mail: xskoupy1@node.mendelu.cz